Novel Synthetic Methods

Mater. Res. Soc. Symp. Proc. Vol. 1309 © 2011 Materials Research Society
DOI: 10.1557/opl.2011.97

Superconducting Parent Compound Pr_2CuO_4 Achieved by Special Post-Reduction

Hideki Yamamoto[1], Osamu Matsumoto[2], Keitaro Yamagami[1], Michio Naito[2], and Yoshiharu Krockenberger[1]
[1]NTT Basic Research Laboratories., NTT Corporation, Atsugi-shi, Kanagawa, 243-0198, Japan
[2]Department of Applied Physics, Tokyo University of Agriculture and Technology, Koganei-shi, Tokyo, 184-8588, Japan

ABSTRACT

It is commonly believed that the parent compounds of high-T_c cupratres are, universally, charge transfer insulators and triggered by Mott physics. In our experiments using metal-organic decomposition (MOD), however, accumulating evidences show that the parent compounds of "electron-doped" superconductors, $RE_{2-x}Ce_xCuO_4$ [RE = rare earth ion] with x = 0, are not Mott insulators but superconductors [1-5]. They have a T_c of 30 K and crystallize in the Nd_2CuO_4 (T') structure. Most likely, the sharp contradiction between our results and commonly achieved data originates from the complicated oxygen chemistry in these materials. The as-synthesized specimens contain a fair amount of impurity interstitial oxygen. Throughout the reduction process it is required to remove exclusively impurity oxygen while preserving regular oxygen site occupied in order to obtain superconductivity. With decreasing x the constraints of the reduction process are getting more tight. In this study, we systematically investigated the post-annealing process using MBE-grown T'-Pr_2CuO_4 films. The MBE films were reduced *ex-situ* in a tubular furnace following a specially designed 2-step process, as in the case of MOD films. The films were annealed at T_a = 700 - 850°C in a reducing atmosphere (P_{O2} = 2 x 10^{-5} - 2 x 10^{-3} atm) and finally reduced at a lower temperature T_{red} = 450 – 700°C under vacuum (< 10^{-4} Torr). The film properties systematically changed with T_a, P_{O2}, and T_{red}. The optimized T_{red} varies from 475°C to 650°C mainly depending on T_a, since the microstructure and grain size of the films are determined by T_a. Optimal superconducting properties are T_c of 26 K, while ρ(300 K) = 250 μΩcm, and RRR ~ 10. We believe the combination of thin-film synthesis and specially designed post-reduction process enabled us to obtain nearly intact CuO_2 planes. Samples prepared by above-mentioned method unveiled the intrinsic properties of the parent compounds, which are not triggered by Mott physics. This result also agrees with the recent calculation result indicating the parent compounds with T' structure are not charge transfer insulators [6-8].

INTRODUCTION

Recently, grain boundary/size engineering is getting a more and more popular concept in the field of solid state ionics [9], where research on ionic conduction itself is essential to improve the performance of, e.g., batteries. Here, we show such an approach gives an important clue to understand still puzzling electronic properties and the electronic phase diagram of high-T_c cuprate superconductors. Cuprate superconductors are the record holder in T_c [10]. The electronic phase diagram of the cuprates, however, remains enigmatic and is a key ingredient to understand the mechanism of high-T_c superconductivity. Due to the apparent and rough "electron-hole" symmetry in the phase diagram [12], the doped Mott insulator scenario has been widely accepted, in which the parent compound is a charge transfer insulator triggered by Mott physics. High-T_c superconductivity develops when the insulator is exposed to doping either by

holes or electrons. However, one should bear in mind that the argument for the "electron-hole" symmetry is based on a comparison of doping in different structures, namely, hole doping in the K_2NiF_4 (*T*) structure [e.g., $La_{2-x}Sr_xCuO_4$ (LSCO)] and electron doping in the Nd_2CuO_4 (*T'*) structure [e.g., $Nd_{2-x}Ce_xCuO_4$ (NCCO)]. The Cu-O coordination in these two structures is significantly different: octahedral CuO_6 in *T* and square-planar CuO_4 in *T'*. On the hole doping side, most experimental results show good coincidence with each other and the phase diagram is established to a large extent [13]. However, on the electron doping side, reported data are still quite controversial and the observed properties strongly depend on material specific parameters such as sample preparation [14,15] and constituent *RE* element [16-20]. Such sample dependent fluctuations arises from a complicated oxygen chemistry in the *T'*-cuprates, in that superconductivity is achieved only after removal of a tiny amount of oxygen (~1%) from the as-synthesized specimens through a post-annealing (reduction) process. More strictly, the constraints are to remove exclusively non-stoichiometric oxygen while preserving regular oxygen sites occupied throughout the reduction process. The complicated annealing process demonstrates that fluctuations in sample properties cannot be ruled out for various methods. Therefore, the optimization of the reduction process must be performed first at each doping concentration *x* in order to establish the generic phase diagram [21-22].

Regarding the doping dependency of the reduction process, it is known that the sample properties become increasingly sensitive to the reduction process with decreasing *x* [14,15, 22]. Our recent observation of superconductivity in the parent compounds of *T'*-RE_2CuO_4 [*RE* = rare earth ion] is an extreme case of the dependency of the reduction process [1-4]. Furthermore, preparation of $Nd_{2-x}Ce_xCuO_4$ by using the same method over a wide *x* range has revealed that superconductivity is observed for $0.2 > x \geq 0$ with an increase in T_c while the doping concentration *x* decreases [4]. Although the physics behind these observations is not yet fully understood, these results urge an essential revision of the commonly believed phase diagram of electron doped cuprates. Hence, it is imperative that an easy reproduction of superconducting parent-and/or under-doped samples becomes feasible irrespective of an adopted synthesis method. Superconducting parent compounds have been obtained reproducibly by MOD technique and systematically investigated though success remains elusive by applying other synthesis methods [23]. Nonetheless, trivalent substitution, $(La,RE)_2CuO_4$ [23-26], has been applied successfully. In this study, we systematically investigated synthesis- and post-annealing processes using MBE-grown *T'*-Pr_2CuO_4 films in order induce superconductivity. As a results, superconducting parent compound Pr_2CuO_4 can be prepared irrespective of the synthesis route by systematic optimization of the post-annealing conditions, in which microstructure and grain size of the films are taken into account.

EXPERIMENT

Epitaxial *T'*-Pr_2CuO_4 thin films were grown in a custom-designed MBE chamber (base pressure ~ 10^{-9} Torr) from metal sources by using multiple e-gun evaporators together with an atomic oxygen (0.5 sccm) source activated by rf at a power of 250 W [27]. The cation stoichiometry adjustment was performed by controlling the evaporation beam flux of each constituent element by means of electron impact emission spectrometry (EIES) via a feedback loop to the e-guns. The growth temperature T_s was varied between 500 and 650°C for the

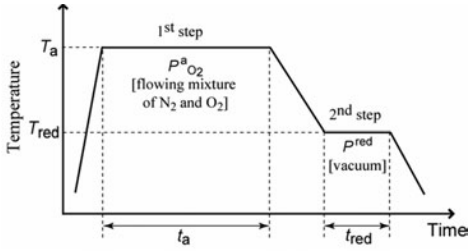

Figure 1. Post-annealing sequence in vacuum tubular furnace. The *ex-situ* annealing process is composed of two steps. In the 1st step, the films are annealed in a reducing atmosphere at relatively high temperature T_a, followed by the 2nd step reduction in vacuum, which is performed at a lower temperature T_{red}.

epitaxial films, which provides us epitaxial films with various grade of crystallinity. The films were grown mainly on $SrTiO_3$(100) substrate. The thickness of the Pr_2CuO_4 films is 1000 Å.

A special 2-step *ex-situ* furnace-annealing process was adopted, similar to MOD synthesis of superconducting Pr_2CuO_4 [1-5] (Fig. 1). In the 1st step, the films were annealed in a reducing atmosphere. The annealing time t_a (60 min) was kept constant while the annealing temperature T_a (700 - 850°C) as well as the partial oxygen pressure P^a_{O2} ($9 \times 10^{-5} - 2 \times 10^{-3}$ atm) have been varied. During the second step the reduction temperature T_{red} was systematically varied and the annealing time t_{red} (10 min) was kept constant. During the 2nd reduction step the furnace was evacuated (<10^{-4} Torr) and kept under vacuum until the furnace reached 150°C. Note that an *in-situ* UHV annealing process, which gives superconducting properties of $T_c \sim 25$ K, ρ(300K) ~ 100 μΩcm for MBE-grown $Pr_{1.86}Ce_{0.14}CuO_4$ thin films [28], was insufficient to induce superconductivity into the parent compound Pr_2CuO_4.

RESULTS AND DISCUSSION

Figure 2(a) shows the influence of the temperature during the 2nd annealing step T_{red} on the ρ - T characteristics of the Pr_2CuO_4 films. The films were grown by MBE at T_s = 600°C and subsequently annealed at T_a = 850°C and $P^a_{O2} = 2 \times 10^{-3}$ atm (1st step). With increasing T_{red}, the resistivity value decreases and T_c increases until T_{red} = 650°C. Further increase in T_{red} up to 700 °C causes an abrupt increase of resistivity and superconductivity vanishes.

Next, we examined the influence of T_{red} for the films annealed at different T_a (and P^a_{O2}) in the 1st annealing step. Figure 2(b) shows ρ - T curves of our optimized films so far obtained for different T_a. Almost independently of T_a, the films have a low resistivity of ρ(300K) ≤ 300 μΩcm and high $T_c \sim 26$ K. However, the optimal 2nd annealing step temperature T_{red}^{opt} showed significant dependency on T_a; namely, T_{red}^{opt} = 475°C for T_a = 750 °C while T_{red}^{opt} = 650°C for T_a = 850 °C. In order to obtain a clue to understand the observed deviation in T_{red}^{opt}, AFM (Atomic Force Microscopy) images were taken. Figure 4 shows typical AFM images of the Pr_2CuO_4 films: (a) as-grown with T_s = 600°C, (b) after the 1st step annealing at T_a = 750°C, and (c) after the 1st step annealing at T_a = 850°C. Grains of approximately 800 Å diameter (comparable to thickness) are formed. After the 1st annealing step at T_a = 750°C, the average grain size increases up to 2000 Å diameter [Fig. 3(b)]. For films annealed at T_a = 850°C, the surface morphology is

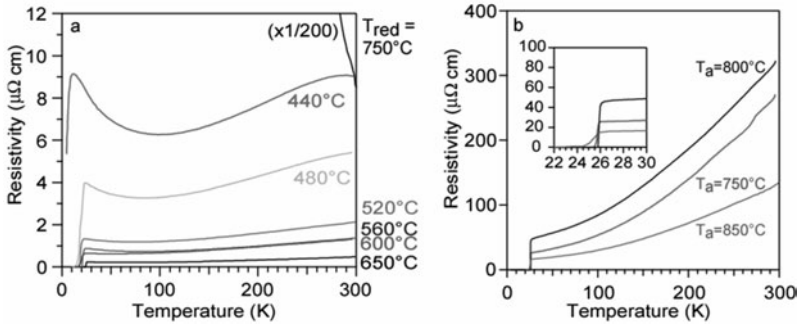

Figure 2. (a) Plot of ρ - T curves of Pr_2CuO_4 films reduced at various temperature T_{red} in the 2nd annealing step. (b) The best-optimized ρ - T curves of Pr_2CuO_4 films annealed in the 1st step at different T_a. The optimal temperature T_{red}^{opt} in the 2nd step is different depending on T_a.

reminiscent to a step-and-terrace structure with larger domains [Fig. 3(b)]. Note, that the microstructure and morphology of the films did not change after the 2nd reduction step performed at T_{red} < 650°C. The above observation provides qualitative explanation for the dependency of T_{red} and T_a on the transport properties. We assume that not only out-of-plane but also in-plane diffusion of oxygen play an essential role in determining oxygen composition and configuration in the resultant films. This surmise is consistent with the fact that the optimal reduction temperature is ~ 450°C in the MOD films, in which the typical grain size is smaller (≤ 1000 Å) than that of the MBE-grown films [5].

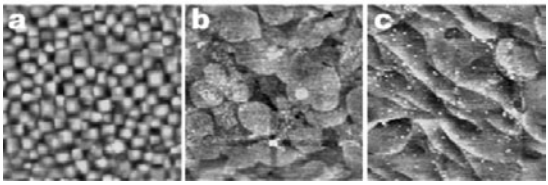

Figure 3. AFM images (1x1 μm^2) of the Pr_2CuO_4 films: (a) as-grown with T_s = 600°C, (b) after the 1st annealing step annealing at T_a = 750°C, and (c) after the 1st annealing step at T_a = 850°C. The grain size of the as-grown film is around 800 Å. Through the 1st step annealing at T_a = 750°C, the grain size increases up to ~ 2000 Å with a change in shape. For the film with T_a = 850°C, the grain size further increases and the surface structure is reminiscent of a step-and-terrace structure.

CONCLUSIONS

We systematically investigated the synthesis- and post-annealing process using MBE-grown T'-Pr_2CuO_4 films. Superconducting specimens were obtained by a specially designed 2-

step annealing process by optimizing the annealing parameters. Optimal superconducting properties are T_c of 26-27 K, while ρ(300 K) = 250 μΩcm. The observed T_c of the parent compound Pr_2CuO_4 is higher than that reported for any electron-doped $Pr_{2-x}Ce_xCuO_4$. The present study indicates that superconductivity in Pr_2CuO_4 films can be obtained by tuning the post-annealing process independently of the crystalline quality of the as-grown films. This opens the way for synthesizing superconducting Pr_2CuO_4 films by other methods.

ACKNOWLEDGMENTS

The authors thank H. Shibata, Y. Taniyasu, and T. Akasaka for their supports in experiments.

REFERENCES

1. O. Matsumoto, A. Utsuki, A. Tsukada, H. Yamamoto, T. Manabe, M. Naito, Phys. Rev. B **79**, 100508(R) (2009).
2. O. Matsumoto, A. Tsukada, H. Yamamoto, T. Manabe, M. Naito, Physica C **468**, 1148 (2008).
3. M. Naito, O. Matsumoto, A. Utsuki, A. Tsukada, H. Yamamoto, T. Manabe, J. Phys. CS **108**, 012037 (2008).
4. O. Matsumoto, A. Utsuki, A. Tsukada, H. Yamamoto, T. Manabe, M. Naito, Physica C **469**, 924 (2009); *ibid*, **469**, 940 (2009).
5. O. Matsumoto, A. Tsukada, H. Yamamoto, T. Manabe, M. Naito, Physica C **470**, 1029 (2010).
6. H. Das, T. Saha-Dasgupta, Phys. Rev. B **79**, 134522 (2009).
7. C. Weber, K. Haule, G. Kotliar, Nat. Phys. **6**, 574 (2010).
8. C. Weber, K. Haule, G. Kotliar, Phys. Rev. B **82**, 125107 (2010).
9. J. Maier, Nat. Mater. **4**, 805 (2005).
10. S. Uchida, J. Phys. Soc. Jpn. Suppl. C **77**, 9 (2008).
11. H. Hosono, Physica C **469**, 314 (2009).
12. M. B. Maple, MRS Bulletin **15**, 60-67 (1990).
13. H. Takagi, T. Ido, S. Ishibashi, M. Uota, S. Uchida, Y. Tokura, Phys. Rev. B **40**, 2254 (1989).
14. M. Brinkmann, T. Rex, H. Bach, K. Westerholt, Phys. Rev. Lett. **74**, 4927 (1995).
15. M. Brinkmann, H. Bach, K. Westerholt, Physica C **292**, 104 (1997).
16. T. Yamada, K. Kinoshita, H. Shibata, Jpn. J. Appl. Phys. **33**, L168 (1994).
17. Y. Koike, A. Kakimoto, M. Mochida, H. Sato, T. Noji, M. Kato, Y. Saito, Jpn. J. Appl. Phys. **31**, 2721 (1992).
18. M. Naito, M. Hepp, Jpn. J. Appl. Phys. **39**, L485 (2000).
19. A. Sawa, M. Kawasaki, H. Takagi, Y. Tokura, Phys. Rev. B **66**, 014531 (2002).
20. S. Li, S. Chi, J. Zhao, H. –H. Wen, M. B. Stone, J. W. Lynn, P. Dai, Phys. Rev. B **78**, 014520 (2008).
21. P. Richard, M. Neupane, Y. -M. Xu, P. Fournier, S. Li, P. Dai, Z. Wang, H. Ding, Phys. Rev. Lett. **99**, 157002 (2007).
22. M. Brinkmann, T. Rex, S. Markus, H. Bach, K. Westerholt, Physica C **269**, 76-82 (1996).

23. H. Yamamoto, A. Tukada, O. Matsumoto, M. Naito, Physica C, doi:10.1016/j.physc.2009.10.077 (2009).
24. A. Tsukada, Y. Krockenberger, M. Noda, H. Yamamoto, D. Manske, L. Alff, M. Naito, Solid State Commun. **133**, 427-431 (2005).
25. W. Yu, B. Ling, P. Li, S. Fujino, T. Murakami, I. Takeuchi, R. L. Greene, Phys. Rev. B **75**, 020503(R) (2007).
26. L. Zhao, G. Wu, R. H. Liu, X. H. Chen, Appl. Phys. Lett. **90**, 072503 (2007).
27. M. Naito, H. Sato, H. Yamamoto, Physica C **293**, 36 (1997).
28. M. -S. Kim, J. A. Skinta, R. Lemberger, A. Tsukada, M. Naito, Phys. Rev. Lett. **91** 087001 (2003).

Mater. Res. Soc. Symp. Proc. Vol. 1309 © 2011 Materials Research Society
DOI: 10.1557/opl.2011.198

Controlled Hydrothermal Synthesis of Complex Mixed Oxides Using Solution Redox Chemistry

Richard I. Walton,*[1] Kripasindhu Sardar,[1] Helen Y. Playford,[1] Deena R. Modeshia,[1] Richard J. Darton,[1] Janet Fisher[2] and David Thompsett[2]

[1]Department of Chemistry, University of Warwick, Coventry, CV4 7AL, United Kingdom.

[2]Johnson Matthey Technology Centre, Blounts Court, Sonning Common, Reading, RG4 9NH United Kingdom.

ABSTRACT

We present the results of a study of the solvothermal synthesis of mixed-metal cerium-containing oxides all prepared from $CeCl_3.7H_2O$ at less than 250 ^oC in single step reactions. The use of $NaBiO_3$ in the presence of aqueous NaOH yields fluorite solid solutions $Ce_{1-x}Bi_xO_{2-x/2}$ ($x \leq 0.6$), whereas the use of either H_2O_2 or $NaBrO_3$ as oxidant in the presence of TiF_3 yields a Ce(IV) pyrochlore $(Na_{0.33}Ce_{0.67})_2Ti_2O_7$. With replacement of a fraction of the Ti reagent by Sn(IV) acetate, tin doping is possible in the pyrochlore. The materials have all been assessed for their use in catalysis by performing temperature programmed reduction (TPR) experiments under dilute hydrogen flow. The cerium-bismuth oxides show large and apparently reversible hydrogen uptake, but *in situ* powder X-ray diffraction shows that this is accompanied by phase separation into bismuth metal and CeO_2 that occurs over 5 or more TPR cycles. In contrast, the cerium (IV) titanate pyrochlore shows reversible reduction at low temperature (150 ^oC, after an activation step), which gives the material potential use as a precious metal support for catalysis: such as in the water-gas-shift reaction. Although Sn doping lowers the onset of reduction of the pyrochlore, consistent with an expanded lattice, the materials suffer from collapse to give SnO.

INTRODUCTION

Cerium dioxide, CeO_2, is well-known for its uses in catalysis [1,2], where it has important applications in areas of environmental concern, such as in automotive catalytic converters, and in water gas shift (WGS, the conversion of CO and water to CO_2 and hydrogen). In these situations CeO_2 is used as a redox-active solid support for precious metals: this relies on the oxide storage properties of the materials, that derive from the open fluorite lattice and the ability of cerium to convert reversibly between the +4 and +3 oxidation states [1,2]. There is a considerable drive to produce catalysts that operate at low temperatures with the desire to reduce burning temperatures of fuels, for example, and in the case of WGS the need to improve efficiency in equilibrium where the forward reaction is exothermic. Doping of ceria is an established strategy to tune its redox properties, and a large variety of dopants have been studied, from aliovalent metal ions such as Y^{3+}, Gd^{3+}, Sm^{3+} and Sr^{2+} [3-5], to isovalent metals such as Zr^{4+} [6] and Sn^{4+} [7]. In the latter situation a distortion of the ceria lattice may aid oxide ion migration, and in the former case

this may be coupled with the introduction of a greater concentration of oxide-ion vacancies that enhance oxygen storage. The case of Zr-doped ceria has been particularly well studied [6].

Conventional synthesis approaches to ceria materials for catalysis involve two-step co-precipitation followed by annealing to induce crystallinity. Solvothermal synthesis offers a more versatile approach to synthesis since a one-step crystallisation from solution suggests a means of controlling crystallite size and shape: there are many reports of how solution additives may offer such control over CeO_2 synthesis and its doped variants [8]. We were interested to develop this approach further to study the possible formation of more complex Ce(IV)-containing multinary oxides with a variety of structure types, which themselves have catalytic properties. This follows from a body of work that has shown how complex, mixed-metal oxides may be prepared using hydrothermal chemistry, including perovskites, pyrochlores and spinels whose synthesis would usually be undertaken using traditional solid-state chemistry [9,10]. We were also interested to investigate whether the addition of oxidising agents to hydrothermal synthesis may permit a convenient means of targeting the synthesis of complex oxides with control of oxidation states of constituent metals. This paper contains a brief account of our progress in this endeavour, illustrated with the chemistry of cerium.

EXPERIMENTAL DETAILS

Synthesis

Solvothermal synthesis was performed using Teflon-lined stainless-steel autoclaves with an internal volume of ~20 cm^3. In all reactions the source of cerium was the trichloride heptahydrate, $CeCl_3.7H_2O$. For the preparation of bismuth-doped CeO_2. $NaBiO_3{\cdot}nH_2O$ ($n \sim 2$) was used as oxidant and reagent. In a typical synthesis $NaBiO_3{\cdot}2H_2O$ (85% Acros Organics) and $CeCl_3{\cdot}7H_2O$ (99.9% Alfa Aesar) with desired stoichiometric ratio (based on 2.3 mmol of $NaBiO_3.2H_2O$) were stirred in 4 mL 4 M HNO_3 solution for 10 minutes, to which 4 mL 10 M NaOH was added dropwise with stirring for another 25 minutes. The reaction mixtures were sealed in autoclaves (~50 % fill) which were placed in a pre-heated fan oven at 240 ^oC for 96 hours, before cooling to room temperature. After the reaction orange-yellow precipitates were obtained which were recovered by suction filtration, washed with hot water, and dried at 100 ^oC for few hours. For the synthesis of pyrochlore materials the cerium precursor was reacted in the presence of the metal salts TiF_3 and $Sn(OC_2H_5)_4$ (both Sigma-Aldrich) in the presence of either hydrogen peroxide or $NaBrO_3$ as oxidant and aqueous NaOH (~5 M) at 240 ^oC for 5 hours (50 % fill in the autoclave). A slight excess of Ti:Ce was used (2.5:1) and 50 molar equivalents of H_2O_2. The pale yellow solids were recovered and dried as before.

Characterisation

Powder X-ray diffraction was used both for phase identification and also in the investigation of thermal and redox behaviour. For ambient measurements, a Siemens D5000 diffractometer operating with Cu Kα radiation was used in flat-plate geometry, and for non-ambient measurements a Bruker D8 Advance X-ray diffractometer also operating with Cu Kα radiation but equipped with a VÅNTEC-1 solid-state detector and an Anton-Parr XRK900 chemical reaction chamber was used to allow measurements to be made as a function of temperature and